Mon. Not. R. Astron. Soc. **272,** 80–88 (1995)

# Viscosity prescriptions in accretion discs with shock waves

Sandip K. Chakrabarti[1] and Diego Molteni[2]

[1] *Tata Institute of Fundamental Research, Homi Bhabha Road, Bombay 400005, India*
[2] *University of Palermo, Via Archirafi 36, 90123 Palermo, Italy*

Accepted 1994 August 1. Received 1994 July 28; in original form 1994 March 17

**ABSTRACT**

We study the evolution of viscous, isothermal, rotating, thin, axisymmetric accretion discs around compact objects using smoothed particle hydrodynamics. We emphasize the effects of different choices of viscosity prescription on the evolution of angular momentum, as well as on other physical properties of the disc. We show that a flow with the Shakura–Sunyaev viscosity prescription may produce a mixed shock, where the angular momentum can also change significantly across the shock. We present and study the effects of other prescriptions of viscosity which render the angular momentum continuous across the shock waves. In general, it is observed that, for flows with a small viscosity, the shocks are weaker, form farther away and are wider as compared with the shocks in inviscid flows. If the viscosity is high, shocks do not form at all. The flow remains subsonic and Keplerian throughout the disc and becomes supersonic only very close to the horizon.

**Key words:** accretion, accretion discs – hydrodynamics – shock waves.

## 1 INTRODUCTION

A large number of numerical simulation results present in the literature suggest that shocks may form in adiabatic accretion discs (Hawley, Smarr & Wilson 1984; Chakrabarti & Molteni 1993; Molteni, Lanzafame & Chakrabarti 1994) and in inviscid discs with radiative transfer (Molteni & Sponholz, in preparation). These shock solutions were obtained for inviscid flows and agree with the theoretical predictions (Chakrabarti 1989, 1990a) reasonably well. Chakrabarti (1990b, hereafter SKC90b) discussed the effects of viscosity on the shock formation in isothermal accretion discs around black holes. The general conclusions were that the stable shock ($X_{s3}$ in the notation of SKC90b) is weaker and forms farther away as the viscosity parameter is increased. When the viscosity is very high, shocks do not form at all. Instead, the flow remains subsonic and Keplerian throughout the disc and becomes supersonic close to the black hole after passing through the inner sonic point. In the present paper, we shall study the numerical evolution of viscous isothermal discs, with particular emphasis on the nature of shocks in flows close to a black hole. We show that the solution strongly depends upon the viscosity prescription. In particular, we show that, if the transport of angular momentum follows the Shakura–Sunyaev (1973) $\alpha$-viscosity (hereafter SS$\alpha$) prescription, a mixed shock must form, where a jump of angular momentum takes place. We present other prescriptions in which angular momentum is continuous across the shock waves and, for high viscosity, yields shock-free Keplerian discs exactly as in the Shakura–Sunyaev prescription. These prescriptions, therefore, could possibly be more suitable for discs that include shock waves, as well as for shock-free Keplerian discs.

The plan of our paper is the following. In the next section, we show how different viscosity prescriptions might affect the nature of shock transitions. For simplicity of argument, we consider only *isothermal* flows. In Section 3, we present a test of our code to show that, with a significant viscosity, the disc does become Keplerian. Subsequently, we present a few numerical solutions of the isothermal flows with various viscosity prescriptions, and compare these results. Finally, in Section 4, we summarize our results and draw conclusions.

## 2 MODEL EQUATIONS WITH DIFFERENT VISCOSITY PRESCRIPTIONS

Consider a thin, isothermal, axisymmetric accretion flow on to a compact object. The radial momentum equation is

$$\frac{\partial v_r}{\partial t}+v_r\frac{\partial v_r}{\partial r}+\frac{1}{\Sigma}\frac{\partial W}{\partial r}-\frac{\lambda^2}{r^3}+\frac{\partial \Phi}{\partial r}=0. \tag{1a}$$

The continuity equation is given by

$$\frac{\partial \Sigma}{\partial t}+\frac{1}{r}\frac{\partial}{\partial r}(\Sigma r v_r)=0. \tag{1b}$$

The azimuthal momentum equation is given by

$$\frac{\partial \lambda}{\partial t}+v_r\frac{\partial \lambda}{\partial r}=\frac{1}{r\Sigma}\frac{\partial}{\partial r}(r^2 W_{r\phi}). \tag{1c}$$

Here, $v_r$ and $\lambda$ are the radial velocity and the azimuthal angular momentum respectively, and $W$, $\Sigma$ and $W_{r\phi}$ are the pressure, the density and the $r\phi$-component of the viscous stress tensor respectively. $\Phi(r, \theta)$ is the gravitational potential of the central object. This may be any of the Newtonian or pseudo-Newtonian potentials. For example, $\Phi = -1/2(r-1)$ (Paczyński & Wiita 1980) could be used for flows around a Schwarzschild black hole, or a more complex form (Chakrabarti & Khanna 1992) for flows around a Kerr black hole. All distances, velocities and time-scales are measured in units of $2GM/c^2$, $c$ and $2GM/c^3$ respectively.

If we consider the solution to be steady, the time derivatives of the above equations vanish and we get the following conservation equations.

(i) Conservation of energy:

$$\mathscr{E}=\frac{1}{2}v_r^2+K^2\log\Sigma+\frac{1}{2}\frac{\lambda^2}{r^2}+\Phi. \tag{2a}$$

(ii) Conservation of baryons:

$$\dot{M}=\Sigma v_r r. \tag{2b}$$

(iii) Conservation of angular momentum:

$$\dot{M}(\lambda-\lambda_e)=-r^2 W_{r\phi}. \tag{2c}$$

Here, we have used the polytropic equation of state $W=$ constant $\times\,\Sigma$ appropriate for isothermal flows, and $K=(W/\Sigma)^{1/2}$ is the isothermal sound speed. $\lambda_e$ is the angular momentum at the inner edge of the disc.

A black hole accretion is necessarily transonic (Chakrabarti 1989, 1990a, b). An inviscid flow may be Bondi-like, i.e. may simply pass through a sonic horizon and fall on to a black hole supersonically. As Liang & Thomson (1980) pointed out, however, the flow may have more than one saddle-type sonic point. Subsequently, it was shown that standing shocks may develop in rotating winds and accretion (Habbal & Tsinganos 1983; Ferrari et al. 1985; Fukue 1987; Chakrabarti 1989, 1990a, b). In particular, Chakrabarti (1990b) showed that the topological properties of the phase-space behaviour of the flow depend strongly upon the angular momentum distribution and therefore on the nature of the viscosity.

In an inviscid, axisymmetric flow ($W_{r\phi}=0$), the characteristics (such as the location, strength, etc.) of the shock are determined by the shock conditions (Chakrabarti 1990a, b):

(1) the temperature of the flow is constant across the shock,

$$K_-=K_+; \tag{3a}$$

(2) baryon flux is conserved,

$$\dot{M}_-=\dot{M}_+; \tag{3b}$$

(3) the total pressure is balanced,

$$W_-+\Sigma_- v_{r-}^2=W_++\Sigma_+ v_{r+}^2; \tag{3c}$$

and

(4) angular momentum flux is conserved,

$$\lambda_-=\lambda_+. \tag{3d}$$

Here, $-$ and $+$ signs represent quantiles in the pre-shock and post-shock flows respectively.

In the presence of viscosity, the angular momentum is transported following equation (2c). In the following subsections, we discuss how the transport process depends on the viscosity prescription.

### 2.1 *Shakura–Sunyaev viscosity prescription*

Let us first consider the effects of the SS$\alpha$ prescription. In this case, we have $W_{r\phi}=\alpha_s W(r/\Omega_K)/(\mathrm{d}\Omega/\mathrm{d}r)$, and the angular momentum distribution is obtained from (SKC90b)

$$\lambda-\lambda_e=\frac{\alpha_s r^3 W}{\Omega_K \dot{M}}\frac{\mathrm{d}\Omega}{\mathrm{d}r}=\frac{\alpha_s r K}{M\Omega_K}\frac{\mathrm{d}\Omega}{\mathrm{d}r}, \tag{4}$$

where $M=v_r/K$ is the Mach number of the flow, $\lambda_e$ is the angular momentum at the inner edge of the disc, and $\Omega_K$ is the local Keplerian angular velocity. The subscript s on $\alpha$ denotes the Shakura–Sunyaev $\alpha$-parameter. It is evident that at the shock, since $M$ varies from supersonic ($M_->1$) to subsonic ($M_+<1$), the rate of transport of angular momentum will be different on opposite sides of the shock. In particular, in the post-shock region, the angular momentum will be 'piling' up as the pre-shock flow is unable to transport it away efficiently. Thus the angular momentum must be discontinuous and $\lambda_+$ must be high compared to $\lambda_-$. Thus the shock formed will have the properties of compressional type and shear type. In other words, the shocks will be of mixed type.

### 2.2 *Continuous angular momentum prescriptions*

In the case where the angular momentum is assumed to be continuous across the shock wave, which is reasonable for any axisymmetric flows away from narrow boundaries, one cannot use the SS$\alpha$ prescription. Continuity of $\lambda$ implies continuity of the viscous stress (cf. equation 2c), and one notes that, at the shock (assumed here to be of infinitesimal width),

$$W_{r\phi-}=W_{r\phi+}. \tag{5}$$

In the usual form,

$$W_{r\phi}=\nu\Sigma r\frac{\partial\Omega}{\partial r}. \tag{6}$$

Here, $\nu$ is the kinematic viscosity coefficient, and $\Omega=\lambda/r^2$ is the local angular velocity. Since $\lambda$ is assumed to be smooth and continuous, $\Omega$ is also a smooth and continuous function. One way to achieve the continuity of $\lambda$ across the shock is to define a kinematic coefficient,

$$\nu_p=\frac{\alpha_p(K^2+v_r^2)}{\Omega_K}, \tag{7a}$$

so that the viscous stress is

$$W_{r\phi}=\frac{\alpha_p(K^2+v_r^2)\Sigma r}{\Omega_K}\frac{\partial\Omega}{\partial r}. \tag{7b}$$

In this case, the pressure-balance condition (equation 3c) ensures the continuity of $W_{r\phi}$. This prescription will be referred to as the 'pressure-balanced viscosity prescription'. The subscript p distinguishes this prescription from the other ones.

One could instead use the balance of the mass flux in defining the kinematic viscosity:

$$\nu_{\rm m}=\frac{\alpha_{\rm m}v_r}{\Omega_{\rm K}}, \tag{7c}$$

so that the viscous stress becomes

$$W_{r\phi}=\frac{\alpha_{\rm m}|v_r|\Sigma r}{\Omega_{\rm K}}\frac{\partial\Omega}{\partial r}. \tag{7d}$$

The continuity of the viscous stress follows directly from the conservation of the baryon flux (equation 3b). This prescription will be referred to as the 'mass-flux-balanced viscosity prescription'. The subscript m distinguishes this prescription from the other ones.

### 2.3 *Prescription with flux-limited diffusion*

Recently, the important issue has been raised that, in the boundary layer of a slowly rotating star, the SS$\alpha$ prescription implies that the radial flow has to be supersonic and therefore would lose causal contact with the stellar surface (Narayan 1992). In this situation, the angular momentum is transported rapidly and $\partial\Omega/\partial r$ cannot be a constant. To remedy the problem of causality, a modified form of the kinematic viscosity coefficient was prescribed:

$$\nu_{\rm d}=\alpha_{\rm d}K^2(1-v_r^2/v_{\rm t}^2)^2/\Omega_{\rm K}. \tag{8}$$

Here, $v_{\rm t}\sim\beta a$ (with $\beta$ of the order of unity) is the turbulent speed with which angular momentum is transported fastest. This important modification brings the disc solution into causal contact with the star by enforcing a subsonic accretion. The subscript d distinguishes this prescription from the other ones.

In the case of black hole accretion this specific problem does not arise, since the inner boundary condition dictates that the flow *has to be* supersonic. Also, as in the case of discs in stellar systems, angular momentum transport is not always due to hydrodynamical processes. Radiative, magnetic (e.g. through Alfvén waves) and other transport processes can intervene, and the prescriptions in Sections 2.1 and 2.2 need not be modified any further. The causality argument seems to be a very reasonable one to make (although radiative viscosity can still work); none the less, one wonders if multiplication of $\nu_{\rm p}$ and $\nu_{\rm m}$ as given by equations (7a) and (7c) by a factor $(1-v_r^2/v_{\rm t}^2)^2$ solves the problem. In this case also, $W_{r\phi}$ in the pre-shock flow will be negligible compared with its value in the post-shock flow, and the shock will again become 'mixed-type' and piled-up angular momentum may continuously drive the shock outwards.

## 3 EVOLUTION OF ISOTHERMAL VISCOUS ACCRETION DISCS

In Chakrabarti & Molteni (1993) and Molteni & Sponholz (1994), the basic procedures for the implementation of smoothed particle hydrodynamics (SPH) in cylindrically symmetric coordinates are presented, and it is shown that the simulation results agree very well with the theoretical predictions regarding the shock parameters. In the present paper, we do not discuss this any further. The only modification of the Chakrabarti & Molteni (1993) procedure is the addition of the angular momentum transport equation (1c), with the possibility of using various dynamical viscosity prescriptions as discussed in Section 2 above. As before, we use the Paczyński & Wiita (1980) potential to describe the external Schwarzschild geometry. We note in passing that our code is tested to be free from any numerical viscosity that is shear-type. This is because each of the pseudo-particles is axially symmetric and interacts as a torus.

### 3.1 *Test results*

In Chakrabarti & Molteni (1993), we have already shown that a flow free from viscosity produces shock waves exactly where shock waves are predicted in discs. The code that we use here has been tested for adiabatic flows by Molteni & Sponholz (1994). Here, we first show a test result to indicate that our code is good enough to produce a Keplerian isothermal disc as well. The evolution of a ring of matter into a Keplerian disc in the presence of viscosity was demonstrated long ago (e.g. Pringle 1981). In our simulation, we inject particles at the outer edge of the disc at $r_{\rm o}=100$ with angular momentum 7.00, which is close to the Keplerian value at $r_{\rm o}$. The (constant) sound speed is chosen to be $K=0.005$, and the injection velocity is $v_0=0.003$. The artificial viscosity parameters are $A=1$ and $B=1$ (see Chakrabarti & Molteni 1993, where these parameters are denoted by $\alpha$ and $\beta$). The SPH parameters are particle size $h=0.4$ and particle separation $\delta_{\rm p}=0.2$ (see e.g. Monaghan 1992 for definitions). The viscosity slowly works on the flow and transports the angular momentum outwards, which enables matter to fall on to the central black hole. Particles reaching beyond the outer grid, as well as those below $r=1.3$, are removed. In this way, particles with higher angular momentum are removed from the outer edge, and particles with lower angular momentum are swallowed by the black hole. Figs 1(a) and (b) show the angular momentum distribution achieved after the flow becomes steady. Fig. 1(a) is the result of a simulation using the SS$\alpha$ prescription (equation 4), and Fig. 1(b) is the result of a simulation using the mass-flux-balanced viscosity prescription (equation 7d). The $\alpha$-parameters chosen are $\alpha_{\rm s}=\alpha_{\rm m}=0.25$. In each of these figures, there are about 500 particles. In both cases, the final distribution seems to be very close to the Keplerian distribution (dotted curves) until the marginally stable orbit at $r=3$, after which the flow falls freely and supersonically to the black hole. The excellent agreement suggests that the code with the inclusion of viscosity is working very well.

In all the simulation results listed below, we use the following quantities: the outer edge is at $r_{\rm o}=18$; the velocity of sound $K=0.05$; the specific angular momentum $l=1.89$;

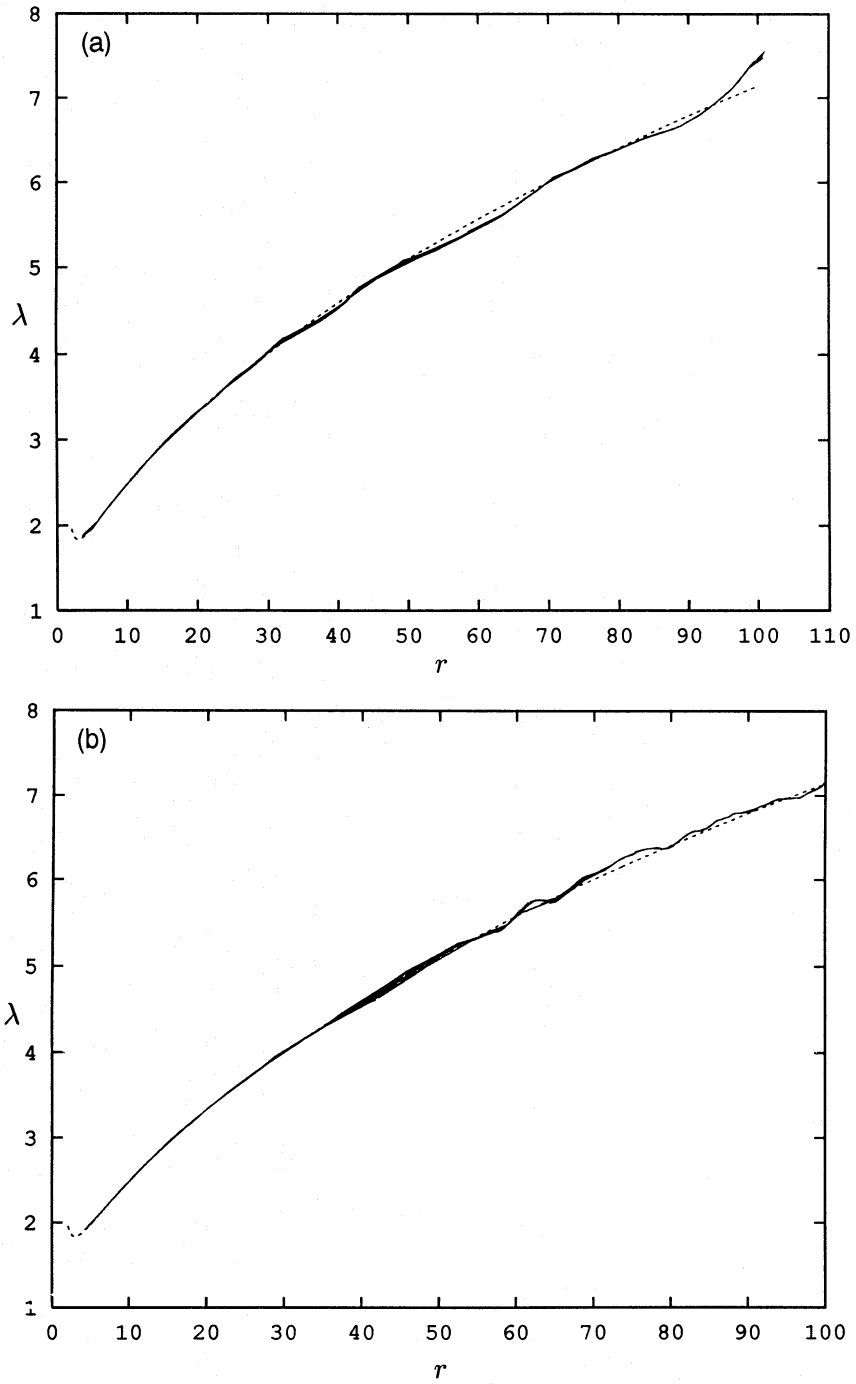


**Figure 1.** Comparison of the Keplerian angular momentum distribution (dotted line) with the distribution obtained by numerical simulations (solid line) using (a) the Shakura–Sunyaev viscosity prescription ($\alpha_s = 0.25$), and (b) the mass-flux-balanced viscosity prescription ($\alpha_m = 0.25$). Thick solid patches are due to denser numbers of particles in some regions.

and the injection velocity $v_0 = 0.1$. Various cases are distinguished by different viscosity prescriptions.

### *3.2 Results obtained using the Shakura–Sunyaev prescription*

In Figs 2(a) and (b) we compare Mach number and angular momentum variations in viscous and inviscid flows. The viscosity parameter $\alpha_s = 0.01$ is chosen everywhere in the viscous disc simulation. Note that the shock in the viscous disc forms farther out and is weaker and wider, as expected (SKC90b). Fig. 2(b) shows that a mixed shock is formed with a jump in angular momentum at the shock ($\lambda_+ > \lambda_-$). This is because the transport rate of angular momentum is higher in the post-shock flow, compared to the rate in the pre-shock flow. The angular momentum is super-Keplerian in the post-shock flow and almost constant in the pre-shock flow.

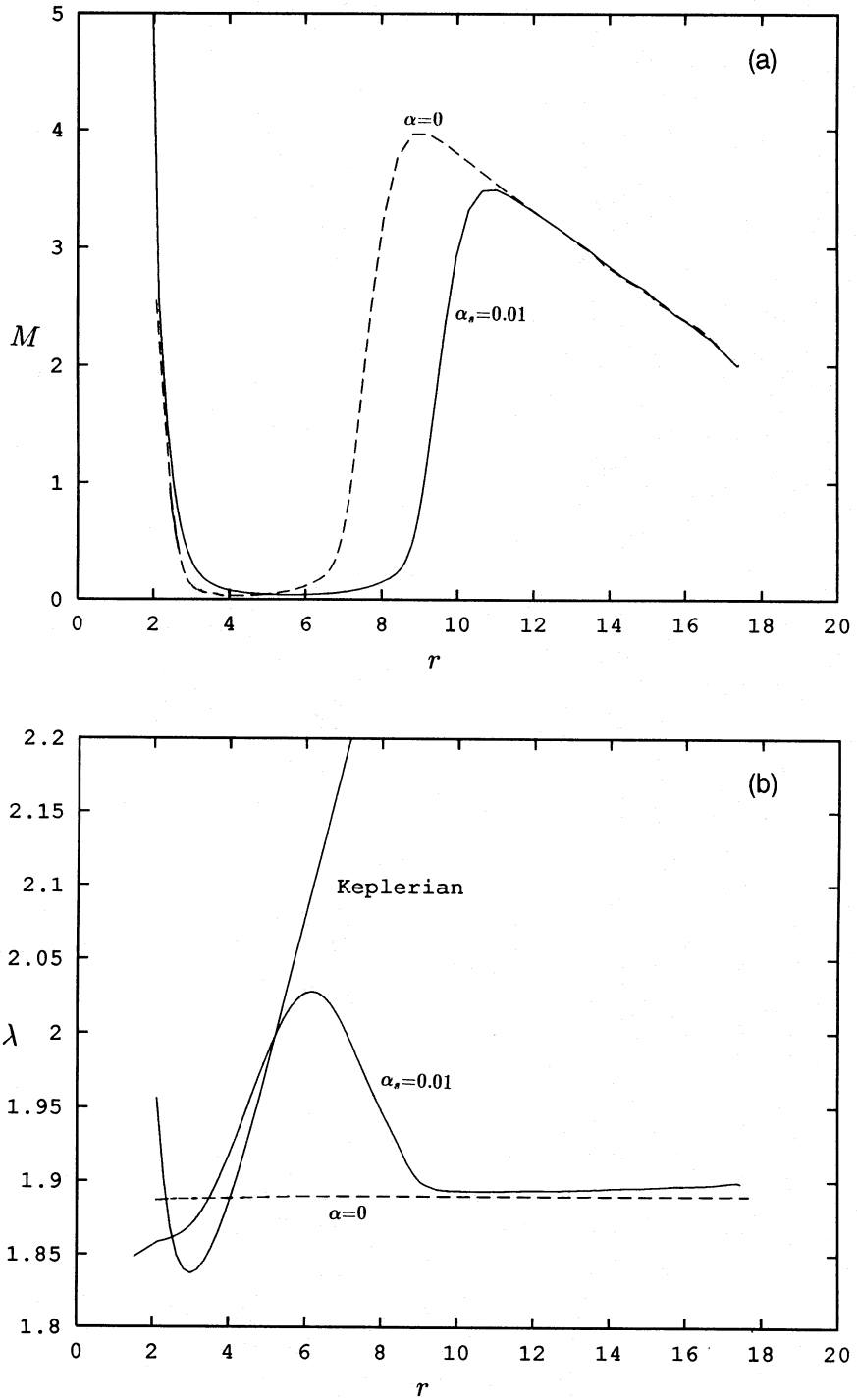


**Figure 2.** Comparison of (a) the Mach number variation and (b) the angular momentum distributions in a disc using the Shakura–Sunyaev viscosity $\alpha_s = 0.01$ (solid curves) with those in an inviscid disc (dashed curves). The shock in the viscous disc is wider, weaker and farther out. In (b), the Keplerian angular momentum is also shown for comparison. Note the super-Keplerian region close to the hole and the angular momentum jump at the shock.

As the $\alpha_s$-parameter is increased, the flow behaviour changes dramatically. Figs 3(a) and (b) show the evolution of Mach number and angular momentum when $\alpha_s = 0.1$ is chosen. One notices that the shock rapidly propagates outwards, making the entire flow outside the inner sonic point subsonic, and the angular momentum distribution resembles more and more the Keplerian one. Successive curves are drawn at intervals of $\Delta t = 500$. The infall time-scale is $t_i = 75$ in the same units. What clearly happens in this case is that the piled-up angular momentum in the post-shock flow drives the shock outwards continuously, and no steady solution becomes possible.

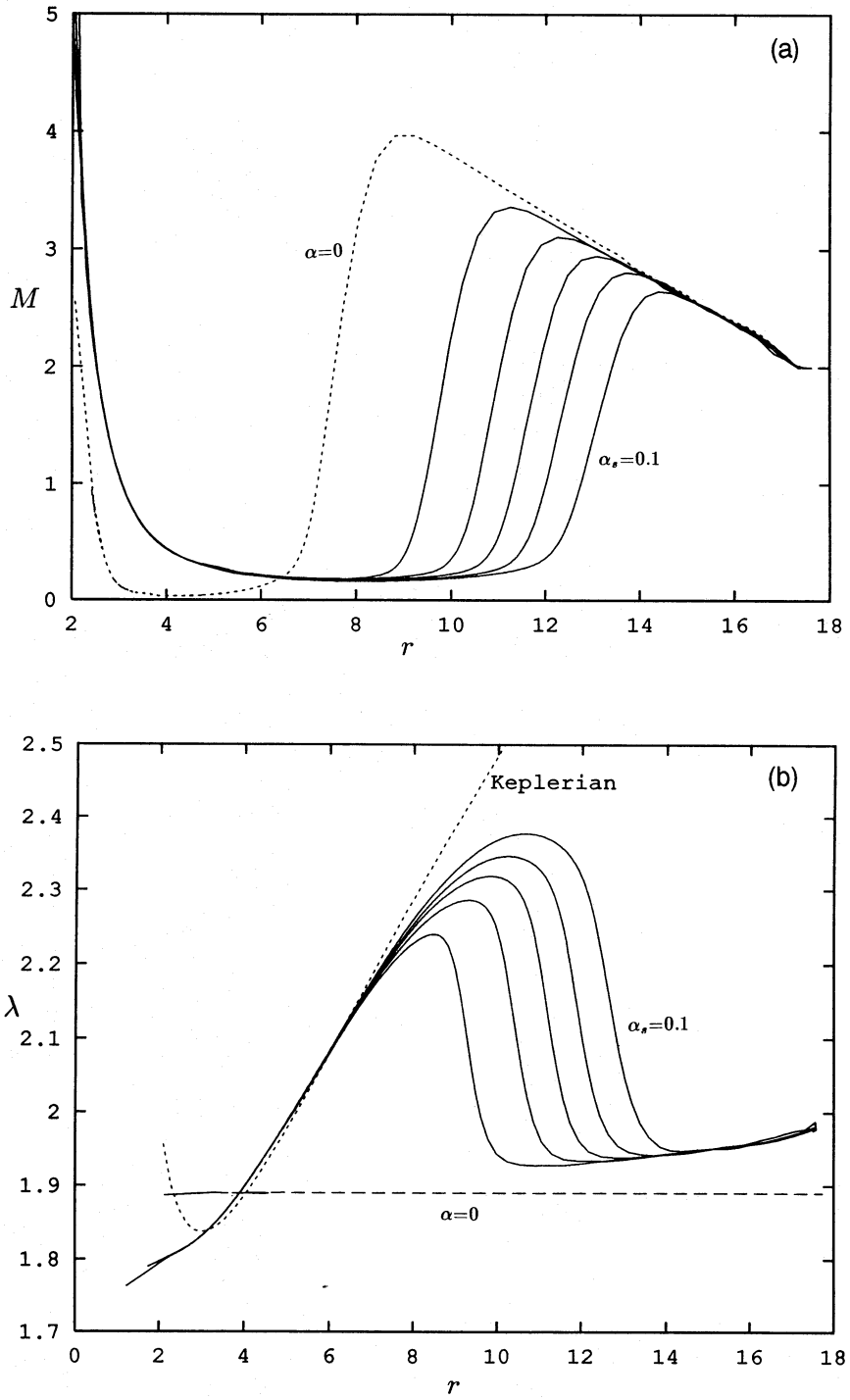


**Figure 3.** Non-steady evolution of (a) the Mach number variation and (b) the angular momentum distribution in a disc with a large Shakura–Sunyaev viscosity ($\alpha_s = 0.1$). Successive curves are drawn at intervals of $\Delta t = 500$ (infall time-scale $t_i = 75$). The shock propagating outwards makes the entire flow subsonic, except in the vicinity of the horizon, and the distribution of angular momentum gradually becomes Keplerian. The steady inviscid disc solution is also presented for comparison.

The topological properties of a viscous accretion flow are discussed in detail by SKC90b, and we do not repeat the discussion here. A salient point that was highlighted is that, when viscosity is very low, a stable and an unstable shock may form (in the notation of SKC90b, at $X_{s3}$ and $X_{s2}$ respectively), with the stable shock ($X_{s3}$) gradually becoming weaker as the viscosity is increased. When the viscosity passes a critical value, the stable shock disappears altogether. Instead, two solutions, both coming from infinity to the horizon, are allowed, none being suitable for a stable shock formation.

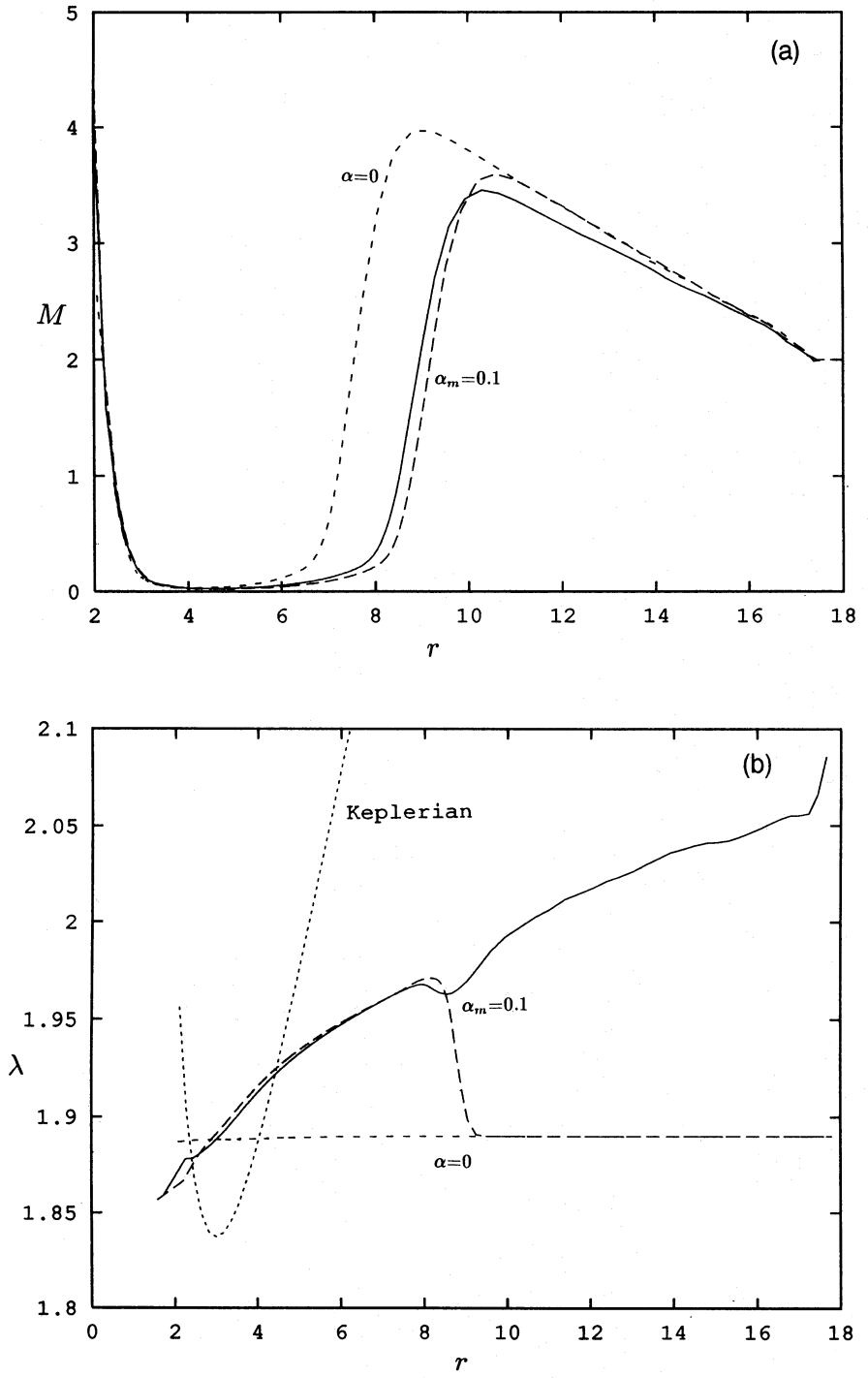


**Figure 4.** Solid curves show (a) the Mach number and (b) the angular momentum distributions of a disc with the mass-flux-balanced viscosity prescription, while long-dashed curves represent flows in which viscosity is suppressed artificially in the supersonic region, following the flux-limited diffusion prescription. $\alpha_m = 0.1$ is used in both cases. Short-dashed curves indicate solutions for inviscid flows. In (b), the Keplerian distribution is provided for comparison.

The solution passing through the inner sonic point has a higher dissipation and entropy (Chakrabarti 1989, 1990a), and is chosen by the realistic flow. Our results presented in Figs 1 and 3 above seem to correspond with this branch of the solution.

### *3.3 Results obtained using the mass-flux-balanced viscosity prescription*

Figs 4(a) and (b) show the variation of Mach number and the angular momentum profile for flows evolved with the mass-

flux-balanced viscosity prescription discussed in Section 2 above. There are three simulation results in each panel of the figure. The solid curve is obtained with $\alpha_m = 0.1$ everywhere, and the long-dashed curve is obtained with $\alpha_m = 0.1$ only in the subsonic region while $\alpha_m = 10^{-6}$ in the supersonic region. This latter case was chosen to mimic the flux-limited diffusion prescription (Narayan 1992). It is clear that the angular momentum distribution is roughly monotonic and sub-Keplerian, except close to the black hole where it is super-Keplerian. The introduction of the flux-limited transport prescription changes the properties of the flow in obvious ways. The shock becomes stronger, but still located farther out. The angular momentum distribution becomes strongly non-monotonic, and the shock is 'mixed-type', where a jump in angular momentum also occurs.

### *3.4 Results obtained using the pressure-balanced viscosity prescription*

Fig. 5 shows the angular momentum distribution of the disc with the pressure-balanced viscosity prescription. The solid curve is obtained with $\alpha_p = 0.1$ everywhere in the flow, and the dashed curve is obtained by using $\alpha_p = 0.1$ in the subsonic region only, while using $\alpha_p = 10^{-5}$ in the supersonic region. The angular momentum distribution is non-monotonic, but is smooth and continuous apart from some numerical noise. In comparison, the dashed curve obtained with the flux-limited transport prescription is smoother. The jump in angular momentum is smaller. The dotted curve represents the Keplerian distribution for reference purposes.

In Fig. 6, we present a comparison of the angular momentum distributions obtained using all of the three prescriptions discussed above. The post-shock flow shows a significant variation of the distribution, while the slopes in the supersonic pre-shock regions remain very similar. Note that $\alpha_p$ is chosen to be an order of magnitude higher than $\alpha_s$ or $\alpha_m$, since the pressure-balanced prescription requires the dynamic viscosity to be proportional to the square of the velocities (equation 7a).

## 4 CONCLUDING REMARKS

In this paper, we have systematically presented the numerical evolution of thin, isothermal accretion discs, following various viscosity prescriptions. We have discovered several significant results. We have found that, when the viscosity is low enough, the shocks are weaker, are wider and form farther out. For high viscosity, the flow does not produce a stable shock, because of a qualitative change in the topological property of the flow. Instead, an unstable shock travels outwards, sweeping the disc and making it subsonic and Keplerian. The flow becomes supersonic only at the inner sonic point, located close to the horizon. These results agree with theoretical expectations (Chakrabarti 1990b). The axisymmetric solutions seem to be stable. In the future, one will need to investigate whether these solutions remain stable under the non-axisymmetric perturbations as well.

We make here the important observation that the Shakura–Sunyaev prescription, regarded widely as the working description of viscosity in accretion discs, does not satisfactorily describe the shocks in the discs, since the shocks are always mixed-type and the jump in the angular momentum produces a region of negative slope (although we do not see any otherwise unpleasant behaviour in terms of stability). In the search for an alternative description, it has become clear

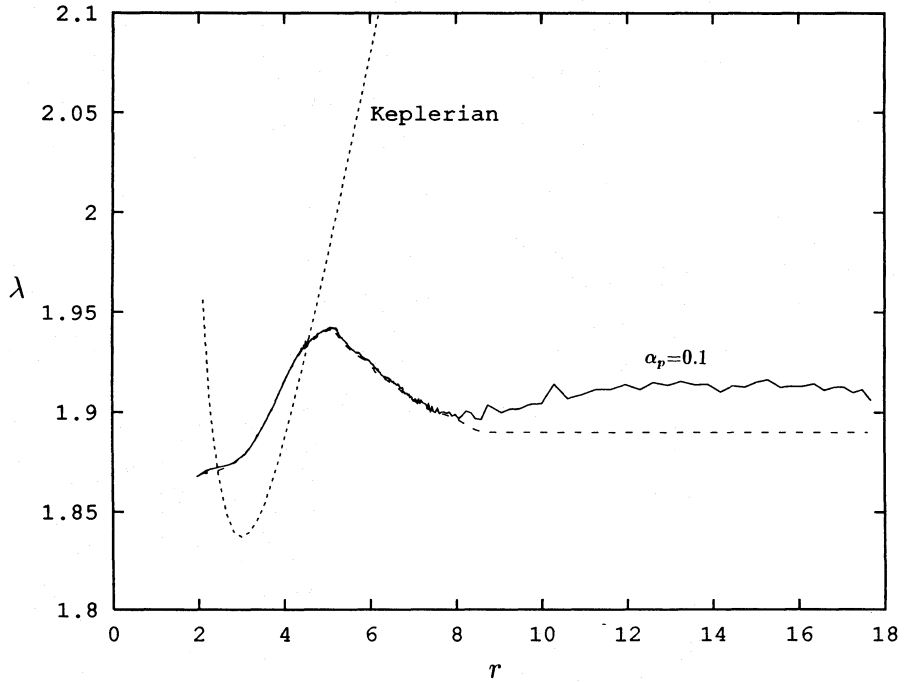


**Figure 5.** Angular momentum distribution of a disc with the pressure-balanced viscosity prescription. The solid curve is for $\alpha_p = 0.1$ everywhere in the flow, and the dashed curve is for $\alpha_p = 0.1$ in the subsonic region but $\alpha_p = 10^{-5}$ in the supersonic region. The dotted curve represents the Keplerian distribution for comparison.

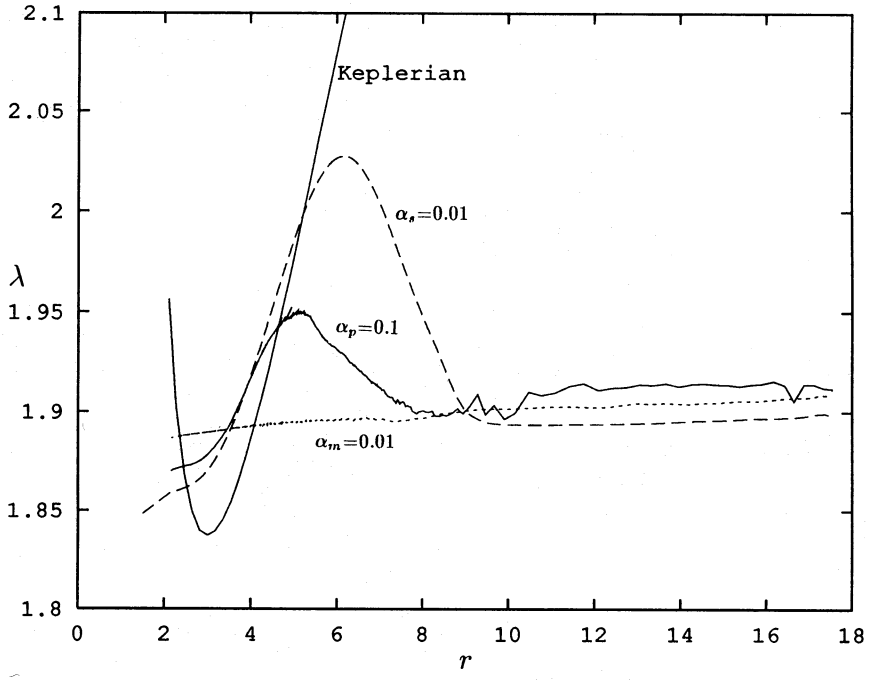


**Figure 6.** Comparison of angular momentum distributions in discs with various viscosity prescriptions: with $\alpha_s = 0.01$ (long-dashed curve); with $\alpha_m = 0.01$ (dotted curve); and with $\alpha_p = 0.1$ (solid, ragged curve). A marked variation occurs only in the post-shock region. A value of $\alpha_p$ was used that was an order of magnitude higher than the values of $\alpha_s$ and $\alpha_m$, since the dynamic viscosity varies as the square of the velocities. The Keplerian distribution (solid, smooth curve) is provided for reference.

that one could instead use the pressure-balance condition or the mass-flux conservation condition to define viscous stress. Each of these prescriptions seems to describe the shocks better. While the pressure-balanced prescription still produces a small jump in angular momentum at the shock, the mass-flux-balanced prescription gives a roughly monotonic, smooth and continuous distribution of angular momentum in the disc, including regions across the shock. When the viscosity is high, this latter prescription reproduces the shock-free Keplerian subsonic solution as well. Thus we believe that the mass-flux-balanced prescription is probably more satisfactory.

The flux-limited diffusion condition, when coupled with any of our prescriptions, produces mixed shocks in the discs, since the viscous stress does not remain continuous. It is possible that, in reality, purely hydrodynamical processes are rare, and the disc angular momentum may be transported via magnetic turbulence or radiative processes. We plan to investigate these issues in more detail in the future.

## REFERENCES

Chakrabarti S. K., 1989, ApJ, 347, 365
Chakrabarti S. K., 1990a, Theory of Transonic Astrophysical Flows. World Scientific, Singapore
Chakrabarti S. K., 1990b, MNRAS, 243, 610 (SKC90b)
Chakrabarti S. K., Khanna R., 1992, MNRAS, 256, 300
Chakrabarti S. K., Molteni D., 1993, ApJ, 417, 671
Ferrari A., Trussoni E., Rosner R., Tsinganos K., 1985, ApJ, 294, 397
Fukue J., 1987, PASJ, 39, 309
Habbal S. R., Tsinganos K., 1983, J. Geophys. Res., 88, 1965
Hawley J. W., Smarr L., Wilson J., 1984, ApJ, 277, 296
Liang E. P. T., Thompson K. A., 1980, ApJ, 240, 271
Molteni D., Sponholz H., 1994, Proc. OAT-SISSA Int. Workshop on Smoothed Particles Hydrodynamics in Astrophysics, in press
Molteni D., Lanzafame G., Chakrabarti S. K., 1994, ApJ, 425, 161
Monaghan J. J., 1992, ARA&A, 30, 543
Narayan R., 1992, ApJ, 394, 255
Paczyński B., Wiita P. J., 1980, A&A, 88, 23
Pringle J. E., 1981, ARA&A, 19, 137
Shakura N. I., Sunyaev R. A., 1973, A&A, 24, 337